Purity and stability of modified nucleosides in the context of accurate quantification by LC-MS

Kira Kerkhoff[1,§], Hagen Wesseling[1,§], Yuyang Qi[1,§], Kuangjie Liu[2], Max Berg[1], Leona Rusling[1], Hendrik Zipse[2] and Stefanie Kaiser[1,*]

[§] these authors contributed equally

* please address your correspondence to stefanie.kaiser@pharmchem.uni-frankfurt.de

[1] Goethe University Frankfurt, Institute of Pharmaceutical Chemistry, Max-von-Laue-Str. 9, 60438 Frankfurt, Germany

[2] Department of Chemistry, LMU Munich, Butenandtstrasse 5-13, 81377 Munich, Germany

Abstract

Reliable quantification of RNA modifications depends on the chemical integrity of synthetic nucleoside standards, yet little is known about their shelf life in aqueous solution. We systematically assessed the short-term stability of 44 canonical and modified nucleosides by LC-UV-MS after storage at -80 °C, -20 °C, 8 °C, 20 °C and 40 °C for up to six months. While canonical nucleosides remained chemically intact, thirteen biologically relevant modifications decomposed in a temperature-dependent manner. 4-thiouridine underwent desulfurisation and dimerisation, 3-methylcytidine deaminated to 3-methyluridine, and N^4-acetylcytidine hydrolysed to cytidine followed by deamination to uridine. mcm^5s^2U displayed desulfurisation, whereas i^6A showed low-level de-prenylation. High-resolution MS established accurate formulas for all degradation products. In order to provide a quantitative basis for nucleoside stability, reaction free energies (ΔG_{298}) for four known decomposition reactions, namely deglycosylation, deamination, deacetylation and desulfurisation, were determined in solution phase quantum chemical calculations. The free energies of these reactions correlate well with the experimental data. All plates remain archived and will be re-analysed at 12, 24 and 36 months to establish long-term rate constants. Our data offer practical guidance for the handling of labile standards and present kinetic parameters that will improve inter-laboratory comparability in RNA modification research.

Introduction

RNA and its four letter-code is expanded in all living organisms by chemical modifications of the major building blocks cytidine (C), uridine (U), guanosine (G) and adenosine (A). Roughly 170 chemical modifications have been reported and collected in the major database MODOMICS so far [1]. Some of these modifications are available as synthetic standards from either commercial sources (Table S1), through chemical synthesis in academic laboratories [2-4] or purification from biological materials [5, 6]. These standards are commonly used by mass spectrometrists in their efforts to (i) unambiguously identify an RNA modification from a biological sample or (ii) quantify its abundance within the sample.

For determination of chemical identity, NMR and high-resolution mass spectrometry are the method of choice. Analytical data is collected on the PubChem database (NIH,[7]). Both technologies give a first indication of contamination with other nucleosides. Regarding purity, HPLC coupled to UV and/or MS detection gives a valuable orientation regarding the presence of isomers of a compound. Here, relative retention times for various RNA modifications are collected at MODOMICS [1]. An even simpler possibility is the use of 2D-thin-layer chromatography using fluorescent cellulose plates followed by UV-detection or radioactivity [8]. The extinction coefficient of ~40 modified nucleosides is known [9] and has been summarized in Table S2. Using this value and a simple (calibrated) photometer, it is possible to assess the concentration of a weighed chemical standard but also of biosynthetically produced standards.

After evaluation of the chemical standard and by using the actual purity value, one can weigh and dissolve the standard to receive a nucleoside stock solution with the ideal working concentration of 10 mM. We, as most other labs, prepare these stock solutions on an irregular basis and store them at either -20 °C or -80 °C, depending on freezer capacity. However, very little is known about the shelf-life of these aqueous stocks. We and others have reported chemical instabilities of modified nucleosides in the past and for some modifications a shelf-life of aqueous stock solutions is reported and summarized in Table 1. For other modified nucleosides, the shelf-life is unknown, and thus past analyses assume that nucleoside stock solutions are stable and can be used long term. This assumption is potentially wrong and thus, absolute quantification of modified nucleosides might be biased. Absolute quantification relies on the use of external calibration using synthetic standards of known concentration. These standards are serially diluted and analysed before or after analysis of the biological samples. If a standard is unstable, the stock concentration decreases and thus a lower signal arises. Yet, the analyst assumes that the signal corresponds to the stock concentration and thus the analyte in the sample suffers from over-quantification. This means that the experimentally

determined value is higher than the true value in the sample. This bias is unknown to the analyst and thus inaccurate data may be received which might bias biological interpretation.

Table 1 Known chemical instabilities of ribonucleosides in aqueous solution		
A known shelf-lives of modified nucleoside chemical standards		
(Modified) ribonucleoside	Shelf life at -20 °C	product
$m^1A(m)$ [10]	3 months [11]	formation of $m^6A(m)$ (dimroth rearrangement)
m^3C [11]	3 months [11]	formation of m^3U
B Known instabilities but no defined shelf-life		
A [12]	Chemical deamination of adenosine to inosine formation	
s^4U [13]	*In-vitro* oxidation using 1 mM iodine leads to s^4U dimer formation	
s^4U [14]	Formation of cytidine in alkaline hydrolysis buffer	
x^5s^2U [14]	In ammonium bicarbonate buffer, formation of (5-modified)-isocytidine	
ct^6A [15, 16]	Ring opening and formation of t^6A, epimerization between hydantoin form (natural) and oxazolone form (potential intermediate in ct6A biogenesis)	
ct^6A [17]	Esterification and glycine addition	

To address the critical but largely unexplored question of how long synthetic nucleoside standards remain analytically reliable, we evaluated the aqueous stability of 44 canonical and modified nucleosides. Using LC-UV-MS we monitored their abundance after storage for up to six months at –80 °C, –20 °C, 8 °C, 20 °C and 40 °C in aqueous solutions. Canonical nucleosides were chemically stable, whereas thirteen modifications showed temperature-dependent decay. Prominent examples include desulfurisation and dimer formation of 4-thiouridine, deamination of 3-methylcytidine to 3-methyluridine, and stepwise hydrolysis and deamination of N^4-acetylcytidine. The wobble nucleoside mcm^5s^2U underwent partial desulfurisation, and i^6A displayed low-level de-prenylation. High-resolution MS confirmed the exact formulas of all degradation products. Quantum-chemical calculations of solution-phase reaction free energies for deglycosylation, deamination, deacetylation and desulfurisation correlated with the experimental trends, providing a predictive framework for untested modifications. Archived plates will be re-analysed after 12, 24 and 36 months to derive long-term rate constants. The resulting kinetic dataset and practical handling recommendations will facilitate robust, inter-laboratory-comparable quantification of RNA modifications.

Materials and Methods

List of chemicals and reagents

All chemicals and reagents were acquired from Merck Chemicals (Darmstadt, Germany) unless stated otherwise.

Quantitative NMR spectroscopy of standards

Nucleosides and internal calibrants were weighed in a suitable sample tube using a Ultramicrobalance XPR2U (Mettler Toledo, Columbus, OH, USA). Both components were dissolved in deuterated solvent and vortexed for 1 min. If dissolution was incomplete, the mixture was additionally sonicated for 15 min. Subsequently, the solution was transferred to Boroeco-5-7 NMR tubes (Deutero GmbH, Kastellaun, Germany) and immediately analyzed using a Bruker AVANCE III spectrometer (800 MHz) equipped with a 5 mm TXO cryoprobe head with z-gradient. The instrument was controlled using TopSpin version 3.6.3. Shimming (TopShim tool 'ts') and probe head tuning and matching ('atma') was applied before each measurement. Key experimental processing and acquisition parameters are listed as follows: nucleus = ^{1}H, number of scans (NS) = 4, receiver gain (RG) = determined before each measurement ('rga'), relaxation delay (D1) = 63 s, pulse width (P1) = determined before each measurement ('pulsecal'), acquisition time (AQ) = 7.7 s, spectral width (SW) = 17.0 ppm, time domain (TD) = 128 000, spectrum size (SI) = 132 000, apodization function = [em], line broadening factor = 0.2 Hz, transmitter offset (O1P) = 4.5 ppm.

Data analysis of quantitative NMR

NMR raw data were processed and analyzed using MestReLab-Software MNova (version 14.1.2). The phase of each spectrum was adjusted manually and baseline corrections were done using the software's polynomial fit algorithm. Integration limits of each signal were set to 0.05 ppm from the ^{13}C satellite signals. The purity of the analyte/nucleoside was calculated using the following equation:

$$P_x = \frac{I_x}{I_{std}} \times \frac{N_{std}}{N_x} \times \frac{M_x}{M_{std}} \times \frac{m_{std}}{m_{sample}} \times P_{std}$$

x = analyte
std = internal calibrant
P = purity (%)
I = integral value
N = number of spins
M = molecular weight (g/mol)
m = weighing amount (g)

For calculations and graph generations, Microsoft Excel and GraphPad Prism software (version 10.4.1) were used.

Weighing nucleoside standards, dilution and preparation before analysis

Nucleoside aliquots between 0.5 mg and 3.0 mg (vendor information in Table S3, exact masses in Table S7) were dispensed into disposable polypropylene weigh boats (PP61.1, Carl Roth, Karlsruhe, Germany) on the same analytical balance as used for NMR analysis. Each aliquot was then transferred to a 1.5 mL polypropylene vial (cat. no. 525-0651, VWR International, Darmstadt, Germany) for subsequent dissolution. The weigh boat was reweighed after transfer, and the net difference was recorded as the precise mass of nucleoside in the vial. Every nucleoside was weighed in triplicate. The spatula was rinsed with ultrapure water and dried with lint-free tissue between samples to prevent cross-contamination. Ultrapure water produced by a Milli-Q Integral system (Merck Millipore, Darmstadt, Germany) was added to each vial to obtain a final nucleoside concentration of 10 mM (Table S7). The contents were vortex-mixed until fully dissolved. For the subsequent stability assay, 20 µL of each 10 mM stock were used to prepare a serial dilution as follows.

1. **First dilution (1 : 10).** Twenty microlitres of the 10 mM stock were pipetted into a 96-well polypropylene plate, followed by 180 µL ultrapure water. The solution was mixed by aspirating and dispensing ten times.

2. **Second dilution (1 : 100).** Twenty microlitres of the 1 : 10 dilution were transferred to a new 96-well plate and combined with 180 µL water, using the same mixing procedure.

3. **Third dilution and master plate preparation (1 : 1000).** One hundred fifty microlitres of the 1 : 100 solution were added to 1350 µL water in a 96 deep-well plate. After thorough mixing, this deep-well plate served as the master plate for all storage conditions.

4. **Aliquoting for storage.** Using an eight-channel pipette set to 100 µL, 30 µL from each well of the master plate were dispensed into individual wells of a standard 96-well plate allocated to the analytical time point. Plates were sealed with aluminium foil, labelled with the designated storage temperature and sampling interval, and immediately placed under the specified conditions.

5. **Start point analysis.** The first plate was immediately analyzed by LC-MS.

Liquid chromatography coupled mass spectrometry

LC-UV-MS experiments were carried out using an Agilent 1290 Infinity II system (Agilent Technologies, Santa Clara, CA, USA), equipped with a diode array detector (DAD) for UV detection and coupled to an Agilent 6470 triple quadrupole mass spectrometer with an Agilent Jet Stream ESI ion source. The DAD wavelengths were set to 254 nm for quantification of original nucleosides and 230nm as well as 320 nm to identify potential degradation products. A volume of 10 µL of each 10 mM nucleoside (100 pmol per inject) solution was injected into the system. Chromatographic separation was performed on a Phenomenex Synergy Fusion-RP column (2.5 µm, 100 Å, 100 × 2 mm; Phenomenex, Torrance, CA, USA) at 35 °C with a flow rate of 350 µL/min. Buffer A consisted of 5 mM ammonium acetate (adjusted to pH 5.3 with glacial acetic acid), and buffer B was Ultra LC-MS grade acetonitrile. The gradient began with 100% solvent A for 1 min, followed by a linear increase to 10% solvent B over 3 min. From 3 to 5 min, solvent B was increased to 40% and held for 1 min, then returned to 100% solvent A over 2 min, followed by a 1 min re-equilibration phase. The mass spectrometer was operated in MS2 scan mode over an *m/z* range of 100 to 600. Data acquisition was done in positive ion mode, with fragmentor voltage set to 90 V and cell acceleration voltage of 5 V.

Data Analysis of LC-UV-MS analysis

Areas of the UV peaks of each sample were integrated and MS2 scans analysed using MassHunter Qualitative Analysis Navigator (Software version B.08.00).

HRAMS analysis

To further investigate nucleosides with observed degradation products, high resolution accurate mass (HRAM) measurements were performed on a Qexactive Plus (Thermo Fisher Scientific, Dreieich, Germany). Fresh and stored nucleoside solutions of ms^2i^6A and mcm^5s^2U and non-stressed nucleoside solution of mcm^5U for comparison, 10 mM each, were diluted to 5 µM in 500:500:1 water/methanol/formic acid and measured on the Qexactive by direct infusion at 5 µL/min into the heated electrospray ionization (H-ESI) source in positive ion mode with a capillary temperature of 320 °C, sheath gas of 10 (nominal units), spray voltage of 4 kV, and an S-lens RF level of 55. Full MS1 scans were acquired for at least 1 min with an AGC target of 1e5 and a maximum injection time of 30 as manual acquisitions in the Thermo Tune software (version 2.9 Build 2926). MS2 and pseudo-MS3 were also acquired for mcm^5U and mcm^5s^2U. Thermo Xcalibur Qual Browser (Thermo Xcalibur v.4.1.31.9) was used to obtain extracted ion chromatograms for each acquisition.

Quantum chemical calculations

Conformational sampling for all systems was performed with CREST 2.12 [18, 19] using the GFN2-xTB [20] method. The structures of all conformers (including those of the most stable tautomers) were subsequently reoptimized at the B3LYP-D3/def2-TZVPP [21-23] level of theory, followed by single point calculations at the SMD(H_2O)/B3LYP-D3/def2-TZVPP [24] level using *Gaussian 09*, rev. D [25]. Refined energies have subsequently been obtained using the DLPNO-CCSD(T)/CBS [26, 27] scheme implemented in ORCA 6.0.0 [28] in combination with the cc-pVTZ and cc-pVQZ basis sets. [29] The DLPNO-CCSD(T)/CBS energies were then combined with solvation free energies in water and thermochemical corrections obtained at B3LYP-D3/def2-TZVPP level to yield final free energies in water at 298.15 K (ΔG_{298}) referenced to a standard state of 1 mol/L.

Results

LC-UV(-MS) analysis reveals impurities in commercial standards

We purchased the 4 canonical nucleosides and 41 modified nucleosides from various vendors and dissolved them in water for a first assessment of purity using LC-UV-MS analysis. While we found that most nucleosides only showed 1 prominent peak, we found 1-methyladenosine (m^1A) to be contaminated with 6-methyladenosine (m^6A) (Figure S1). Furthermore, we found 5-(carboxyhydroxymethyl)-2'-*O*-methyluridine ($mchm^5Um$) to be sold in a mixture of its S- and R-form which complicates quantification (Figure S2, [30, 31]).

Determination of nucleoside concentration using UV or quantitative NMR spectroscopy

Most commercial standards display a purity value in their certificate of analysis. We want to point out that companies claim that their standards are for qualitative analysis only and not for quantitative. Therefore, the indicated purity can be inaccurate and we recommend further quality assurance measures to ensure the purity of the modified nucleosides. For ~ 40 nucleosides, molar extinction coefficients exist (Table S2) which allows quantification by UV absorption. Using the Beer-Lambert law, the concentration of nucleoside solutions can be determined (attention: pH must be correctly adjusted). A comparison of the theoretical concentration and the experimentally determined concentration allows assessment of the nucleoside's purity. A potential confounder would be a UV-active contaminant that absorbs at the same wavelength. Therefore, each measurement in a cuvette should be accompanied with a LC-UV measurement.

For the other modified nucleosides of unknown extinction coefficient (> 90 analytes), we recommend quantitative NMR (qNMR) as an elegant solution to assess the purity of the provided chemical standard. qNMR is considered a relative-primary method, as the integrated signal area is directly proportional to the number of nuclei contributing to the signal and, consequently, to the amount of substance [32]. Typically, an internal calibration method is used, where both the analyte and a standard substance are measured within the same sample, which allows direct referencing of the analyte to the standard within a single spectrum. To achieve results with high metrological quality and the required accuracy, reference standards with certified purity are used [33]. Examples of commonly used ^{1}H NMR certified reference standards for internal calibration are listed in Table S4. These certified standards can be used for high-precision measurements with exceptional accuracy and an overall uncertainty as low as 0.15 % [34].

For quantitative assessments, sample amounts of more than 5 mg are required and complete dissolution in the required 0.5 mL D_2O may be insufficient. An alternative is DMSO-d_6.

One potential issue when using aprotic and/or hygroscopic solvents, such as DMSO-d_6, is that acidic or alkaline protons may lead to broad signals in the spectra, potentially affecting spectral resolution and quantification accuracy. As shown in Figure S3A, the acidic internal calibrant maleic acid (MA) affects the water signal in DMSO-d_6, causing a shift toward higher ppm values and signal broadening. This distortion complicates spectral processing and may lead to biased peak integration and quantification, as seen in the case of 2′-*O*-methyluridine (Um), where signals nearby the broad water peak are directly affected. These issues are not limited to internal calibrants, as acidic or alkaline nucleosides can exhibit similar effects. For instance, as illustrated in Figure S3B, the spectrum of 3-(3-amino-3-carboxypropyl)uridine (acp^{3}U) also shows broad signals. Consequently, to ensure optimal spectral resolution and quantification accuracy, we selected dimethylsulfone (DMS) as the internal calibrant of choice for all subsequent experiments. All subsequent qNMR experiments followed the protocol outlined in the Materials and Methods section and Table S5, beginning with validation of the method by quantifying the purity of DMS using certified MA as an internal calibrant. The results – 99.89% purity in D_2O with an RSD of 0.23 % and 99.98% purity in DMSO-d_6 with an RSD of 0.46% – confirmed both the accuracy and high precision of the qNMR method (Figure 1A).

Next, we applied the same workflow to six different nucleoside standards commonly used for LC-MS-based quantification. The qNMR purity assessment revealed that most of these standards exhibit variations in purity (Figure 1B and Table S6). Um, 4-acetylcytidine (ac^{4}C), and inosine (I) showed purity values ranging between 95% and 99%. As seen in the ^{1}H NMR spectrum of ac^{4}C (Figure S4), unassignable signals are present that cannot be attributed to any protons of ac^{4}C. These signals likely originate from the synthesis process and may indicate

the presence of byproducts or residual solvents detectable by NMR. However, no such unassignable signals were observed in the spectra of the other nucleosides. 5-methyluridine (m^5U) exhibited a purity close to 100%, while acp^3U showed a purity exceeding 110%, and m^2G had a purity below 90%. The unusually high purity value of acp^3U may be explained by the processing issues as already described in Figure S3B. For m^2G, the corresponding ^1H NMR spectrum (Figure S4) indicates no detectable proton-based impurities, suggesting that residual salt from synthesis may contribute to the lower purity value. To investigate this hypothesis, we conducted a proof-of-principle experiment, where we deliberately contaminated the m^5U stock powder with NaCl before sample preparation. The m^5U:NaCl mixture was prepared in a 3:1 ratio, homogenized, and analyzed by qNMR under the same conditions. As shown in Figure 1C, the calculated purity of m^5U dropped to approximately 75%, which supports our idea that residual salts may influence purity assessments. While this experiment does not directly confirm our hypothesis, it suggests that varying nucleoside purities may stem from residual non-^1H-detectable contaminants.

To summarize, we recommend assessment of nucleoside purity if quantitative analysis of biological samples is required. If the extinction coefficient is known, UV absorption measurement in conjunction with LC-UV analysis is advised. For nucleosides of unknown extinction coefficient, we recommend qNMR following the method outlined above.

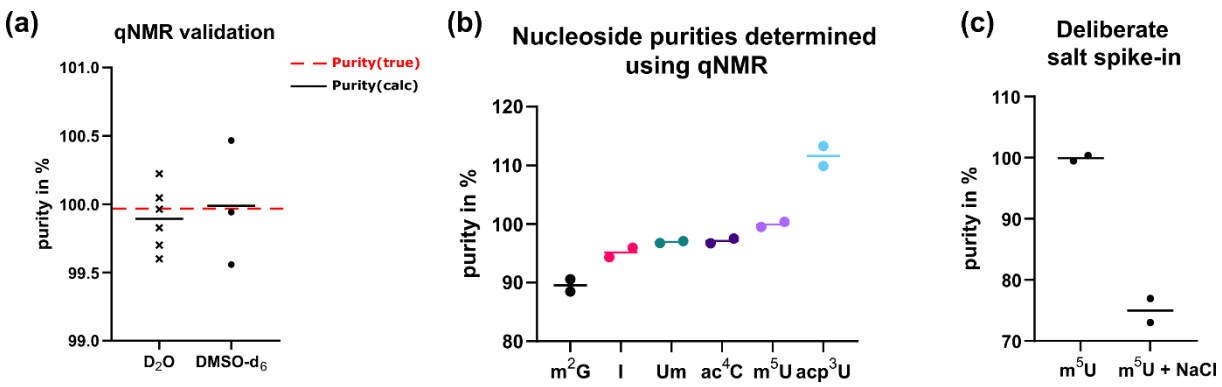

Figure 1 Results of qNMR purity assessment. **(a)** Purity determination of secondary standard DMS (P = 99.96 %) using secondary standard MA (P = 99.93 %) as internal calibrant in D_2O (n = 6) and DMSO-d_6 (n = 3), respectively. Red, dotted line indicates the certified purity of DMS and black lines indicate the calculated purity in D_2O and DMSO-d_6, respectively. **(b)** Purity values of six different nucleoside standards obtained by qNMR (n = 2) **(c)** Purity of m^5U and m^5U which was deliberately contaminated with NaCl.

Determination of nucleoside stability in aqueous solution over 6 months

Preparation of nucleoside solutions

Next, we set out to define the stability of modified nucleosides in aqueous solution. An outline of the study design is given in Figure 2. For this, we reviewed the guideline for stability testing of new drug substances and products (CPMP/ICH/2736/99) from the European Medicines Agency (emea) and we selected the following parameters for testing. -80 °C and -20 °C are considered long-term conditions, 8 °C and 20 °C (often referred to at room temperature, RT) are intermediate conditions and 40 °C was chosen as an accelerated condition for prediction of long-term stability. Due to evaporation at 40 °C, this experiment was only done for the canonical nucleosides and a subset of modified nucleosides previously observed to be instable. Each nucleoside should be analysed in three technical replicates for a minimum time period of 6 months and a maximum time period of 36 months. In total we selected 7 time points and time points 1, 2, 3 and 6 months are included in this manuscript, while time points 12, 24 and 36 months will be reported in 2028. From Table S1 we selected 44 nucleosides and purchased them in quantities above 10 mg. Thus, we were able to weigh each nucleoside three times within a defined mass range of 0.5-3 mg (Table S7). This mass range was selected as it was 5000 times above the partition value which results in a theoretical weighing insecurity below 1 %. Before dissolving the weighed nucleosides in water to a final concentration of 10 mM, two 96-well deep-well plates (2 mL per well; designated as “master plates”) and 58 standard 96-well plates (0.2 mL per well; designated as storage plates) were prepared and labeled according to their intended storage and analysis time points. The nucleosides were then dissolved in water to 10 mM, serially diluted to 10 µM and aliquoted into 58 storage plates and the initial analysis plate. Plates were sealed with aluminium foil and either stored at their respective temperatures or sent to analysis. In parallel, the canonical nucleosides were transferred to cryo-vials and stored at the different temperatures to allow assessment of evaporation from the 96-well plates.

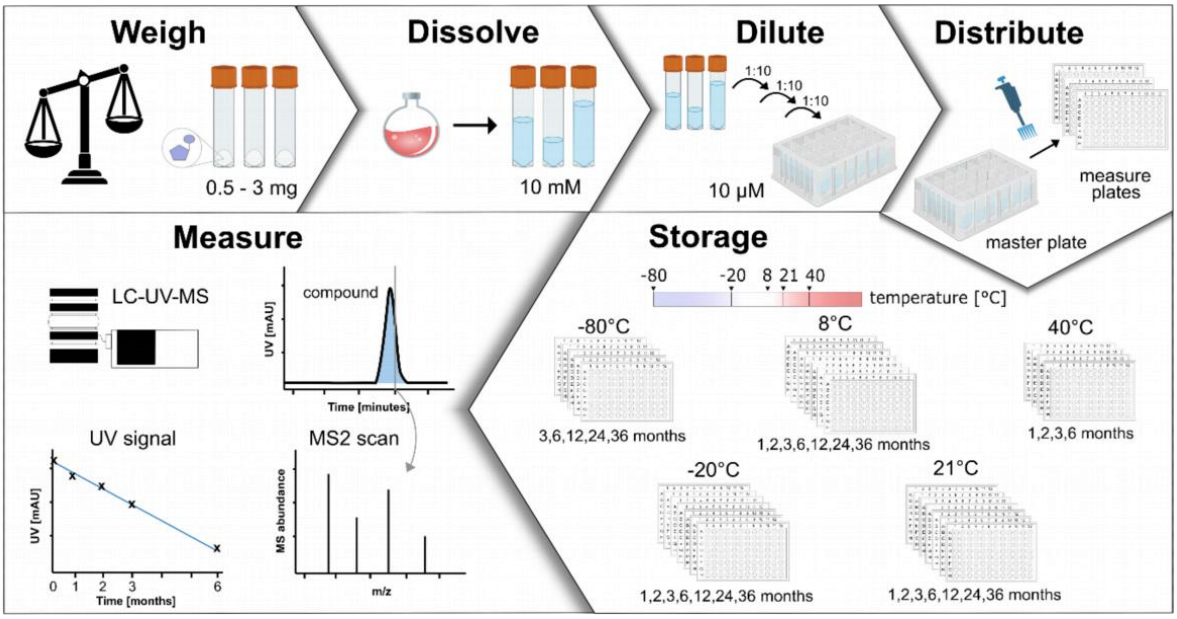

Figure 2 Graphical overview of the study design and workflow which was used to determine the short-term (and long-term) stability of nucleoside solutions. The workflow begins with weighing 0.5–3 mg of compound material into screw top vials, followed by dissolving the compound to a 10 mM concentration. These stock solutions are then serially diluted to 10 µM in master plates and aliquoted into storage plates. Stability of the compound is assessed over time using LC-UV-MS (Liquid Chromatography–Ultraviolet–Mass Spectrometry), with monitoring of its UV signal intensity at 254 nm and mass spectrum (MS2 scan).

Analysis by LC-UV-MS over 6 months

Each nucleoside was injected into a prepared LC-UV-MS system with a 9 minute run time which ensured a runtime of ~ 20 hours per storage condition and a total runtime of 5 days per time point. Each plate stayed in storage until the morning of its use and was then thawed for 1 hour at room temperature followed by a spin-vortex-spin procedure to ensure homogeneity of the analyte solutions. Then the plate was placed in the autosampler at 8°C. Analytes were separated by reverse-phase chromatography and the UV signal at a designated wavelength (see Table S8) was recorded prior to a mass scan ranging from *m/z* 100-600. The UV signal of the analyte and all emerging peaks were integrated and used for monitoring the stability of the nucleosides. The MS scan data from the emerging peaks was analysed to allow first hypotheses on the chemical structures of the decomposition products. After analysis, the plates were discarded.

From the data of time point 0, we calculated the bias introduced at the stage of weighing and serial dilution. Each nucleoside was weighed and diluted in triplicate and from the resulting data we calculated the relative standard deviation (RSD) and we assessed the weighing and dilution accuracy. As shown in Figure S5, the RSD was below 5% for most nucleosides, with 8 nucleosides being between 5-10% and 2 being above 10%.

After 6 months, we calculated the stability of the nucleosides using the UV peak area of each analyte. Time point 0 is considered 100% and used as a reference for the later time points. As a graphical aid, the resulting plots in Figure 3 contain a grey area indicating the deviation from the starting value of +/- 5%, commonly considered to be caused by technical deviations. As can be seen in Figure 3A, the canonical nucleosides are stable over 6 months at all temperatures. Especially at higher temperatures, outlier signals exceeding 100 % occur which indicates evaporation due to inefficient sealing of single wells. However, the use of cryo-vials does not solve randomly occurring evaporation cases. In contrast, our data indicates that our selected cryo-vials are not gas tight and water evaporates systematically, especially at higher temperatures (Figure S6). Thus, we are convinced that our collected data from well-plates is the best technical solution and random outliers caused by evaporation were removed and thus do not impact the results of this study.

9 cytidine modifications were tested for their 6 months stability and 7 can be considered stable at all temperatures (Cm, m^5C, m^5Cm, hm^5C, f^5C, m^4C and m^4Cm). ac^4C was decomposed to 21.8 ± 5% at room temperature and m^3C decomposed at all temperatures, but most pronounced at 8 °C (remaining m^3C is 16.5 ±1%, Figure 3B).

Uridine modifications were more prone to instability and only 5 can be considered stable (Um, Ψ, $m^1Ψ$, m^3U and acp^3U) and 8 showed signs of decomposition within the first 6 months. The bacterial tRNA modification s^4U showed substantial decomposition with a drop to 49.5 ±6.7% even at -80 °C storage (Figure 3C). For m^5U and its ribose-methylated derivative m^5Um, we found a small but consistent decrease in abundance to ~ 92% which might indicate an instability (Figure S7). In tRNA, uridine at position 34 is often modified to fine-tune translation. We had 5 human U34 modifications available and we found that all of them showed clear signs of instability even if stored at - 80 °C. The most pronounced effect was seen for mcm^5s^2U which was unstable at all temperatures but especially at room temperature where only 28.6 ± 14.6% remained after 6 months (Figure 3C). The other four, cm^5U, mcm^5U, ncm^5U, and mcm^5Um, are stable at -20 °C (Figure 3D), indicating that this temperature is optimal for their stability and should neither be exceeded nor reduced (visualized in Figure S8).

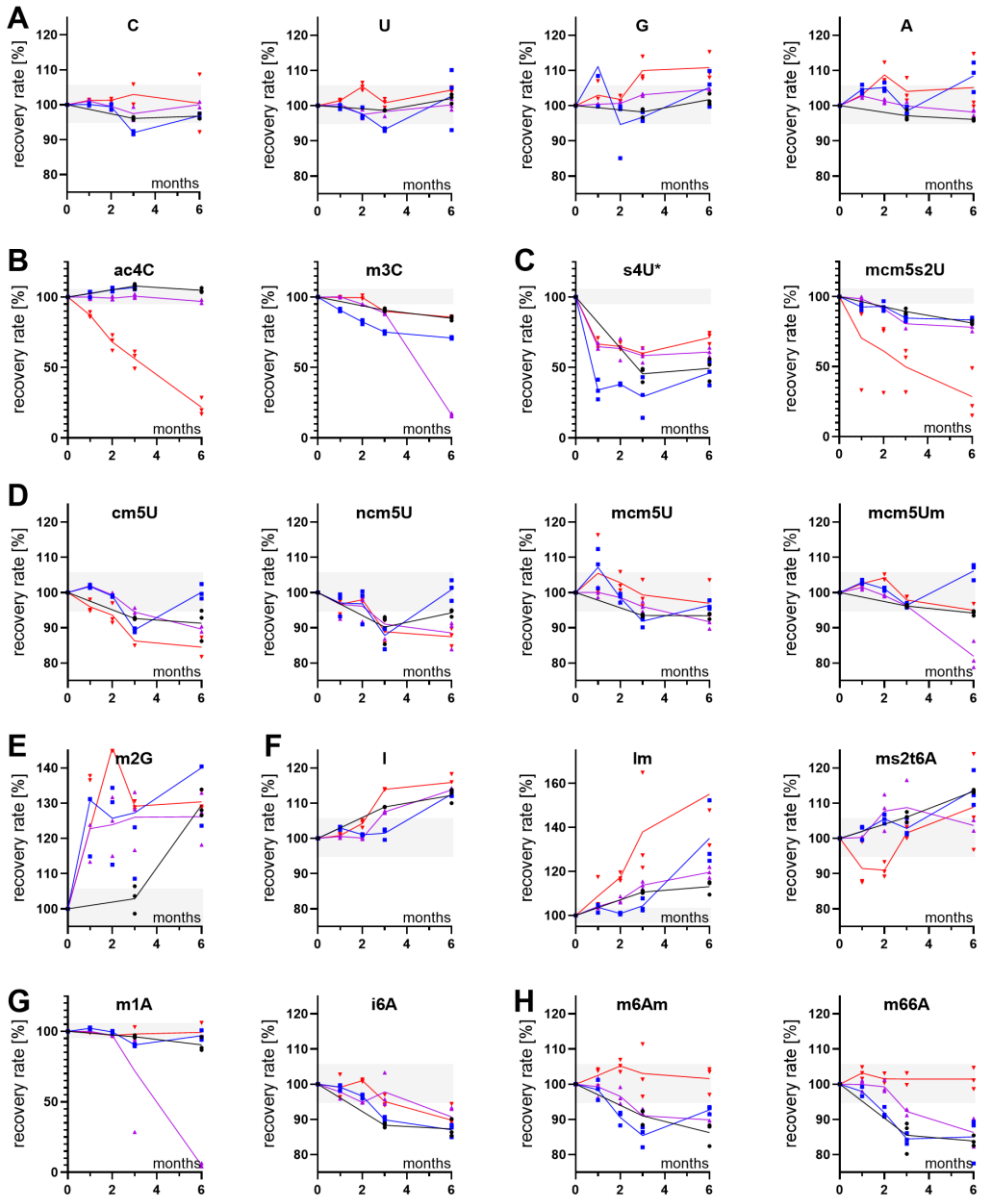

Figure 3 Shelf life of aqueous nucleoside solutions is assessed by LC-UV-MS after storage at pre-selected temperatures. Color code: -80 °C (black), -20 °C (blue), 8 °C (purple) and 20 °C (red) for 6 months. To obtain the recovery rate, the UV area after storage is normalized to the UV area at timepoint 0. Grey area indicates ±5 % deviation from the start value. (**A**) Canonical nucleosides. (**B**) Cytidine modifications with instabilities after storage time of 6 months. (**C**) Uridine modifications with instabilities after storage time of 6 months for all temperatures. (**D**) Hypermodified uridine modifications, which are stable at -20°C. **(E)** Unexpected high recovery rate of 2-methylguanosine (m^2G). **(F)** Unexpected high recovery rate of adenosine modifications. **(G)** Adenosine modifications with instabilities after storage time of 6 months. **(H)** Adenosine modifications, which show reduced recovery for storage temperatures lower than 8°C.

Out of the 5 guanosine modifications studied, 3 can be considered stable (Gm, m^1G and $m^{2,2}G$) and 2 stood out as unstable. The first is m^7G which shows first signs of instability, especially at temperatures higher than 8 °C (Figure S9). The second is m^2G, a modification our laboratory historically struggles with due to continuous over-quantification in purified tRNA isoacceptors such as $tRNA^{Phe}$, which caused exclusion or critical discussion of this modification [35, 36]. In our stability study, m^2G appears to increase over time and after 6 months we find on average 130 % m^2G in all stored solutions independent of the storage temperature (Figure 3E) and the storage vessel (Figure S9). While we have no explanation for this unexpected observation yet, it is an important information for quantification experiments.

Out of the 13 adenosine modifications studied, only Am and m^2A appeared to be fairly stable (Figure S9). For all others we observed issues that can bias quantification. Similar to m^2G, we observed a higher abundance of inosine, Im and ms^2t^6A over time (Figure 3F). As with our observation for m^2G, we cannot explain this unexpected behaviour, but it is important information to consider during analysis of these modifications. Next to m^1A, which is instable due to dimroth rearrangement, we observed that both i^6A, ms^2i^6A, t^6A, m^6A and m^6t^6A are instable reaching around 90 % of their starting signal after 6 months (Figure 3G and Figure S9). m^6Am and $m^{6,6}A$ show a highly interesting behaviour (Figure 3H). Both nucleosides have a reduced abundance at temperatures below 8 °C, while the abundance is unchanged at room temperature. This observation may be connected to our previous report on LC-MS quantification artefacts, where we found that these two modifications tend to get lost during filtration [11]. This loss during filtration is most likely caused by adhesion to the filter and it is reasonable to assume that adhesion plays a role again especially at cold temperatures. Thus, we hypothesize, that m^6Am and $m^{6,6}A$ might adhere to the polypropylene surface of the wells which can be avoided by storing these nucleosides at room temperature.

Figure S10 compares the recovery rates of canonical nucleosides with those of four chemically labile modifications after six months of storage at 40 °C in cryo-vials (accelerated conditions). For cytidine, uridine, guanosine, and adenosine the apparent abundance exceeds the initial value, with mean recoveries ranging from 110 % for cytidine to more than 180 % for adenosine. This is in accordance with our previous observation at lower temperatures (Figure 3A). As an abundance cannot increase in sealed vials, the increase can be attributed either to water loss from the cryo-vials or gradual desorption of nucleosides from plastic surfaces. In contrast, the four modifications exhibit loss profiles that reflect their individual chemical stabilities. The signal for m^2G rises to 110–190 %, indicating that this nucleoside is chemically stable and subject to the same physical concentration effects observed for the canonical nucleosides. ac^4C is no longer detectable, consistent with rapid deacetylation and subsequent deamination. s^4U shows recoveries between 45 % and 65 %, in agreement with parallel desulfurization and dimer

formation. mcm^5s^2U retains approximately 70–80 % of its initial signal, reflecting partial degradation.

These data demonstrate that two distinct phenomena influence quantitative read-outs. First, evaporation and potentially desorption artefacts can yield apparent signal gains for chemically inert nucleosides. Second, genuine chemical decay produces signal losses whose extent depends on the intrinsic reactivity of the modification. For this study, a summary of found instabilities and the consequences for quantification is found in Table 2.

Assessment of degradation products

Quantitative analysis of 4-thiouridine (s^4U) stability over a three-month period revealed rapid degradation across all tested storage temperatures (Figure 4A). LC-UV-MS analysis identified two primary degradation products: uridine (U) and a disulfide-bridged dimer of s^4U (di-s^4U). The relative distribution of these products is temperature dependent. At 8 °C and 20 °C, uridine formation dominates, which is consistent with a desulfurization reaction. In contrast, lower temperatures (-20 °C and -80 °C) favor the formation of di-s^4U, suggesting a radical-mediated mechanism that proceeds via thiol oxidation and disulfide bond formation. These results confirm the pronounced chemical instability of s^4U in aqueous solution and demonstrate that for quantification freshly prepared solutions must be used directly after weighing and dissolution. Storage, even under frozen conditions, is not compatible with reliable quantification.

We also observed a temperature-specific degradation profile for 3-methylcytidine (m^3C). While m^3C remained stable at -80 °C, -20 °C, and 20 °C over six months, a pronounced degradation was observed at 8 °C, where the residual signal decreased to 16.5 ± 1%. LC-UV-MS analysis identified 3-methyluridine (m^3U) as the primary degradation product (Figure 4B). This transformation is consistent with a hydrolytic deamination reaction previously described [11]. The selective degradation at 8 °C, but not at lower or higher temperatures, indicates a distinct chemical vulnerability of m^3C under intermediate storage conditions. Based on these findings, storage at 8 °C should be avoided. Deep-freeze or ambient temperature conditions may be more appropriate, depending on the requirements of the downstream application.

For 6-isopentenyladenosine (i^6A), we observed no instability by only using the quantitative signal graph (left side of Figure 4C), but by analysis of the LC-UV-MS chromatograms we identified a time-dependent conversion into adenosine. MS fragmentation data support the loss of the isopentenyl side chain, showing the disappearance of the $[M+H]^+$ signal at *m/z* 336 and the appearance of a new signal at *m/z* 268 (=adenosine), corresponding to the expected loss of 68 Da. These results indicate a small (less than 5%) but consistent chemical lability of

i^{6}A under prolonged storage, which is masked in the quantitative analysis by an additional evaporation or adsorption effect of i^{6}A.

We next investigated the stability of N4-acetylcytidine (ac^{4}C) under different storage conditions. As shown in Figure 4D, ac^{4}C is chemically unstable and degrades progressively, with the extent of degradation strongly depending on the temperature. At -80 °C and -20 °C, the compound remains largely intact, and the measured signal increases slightly over time. This increase is likely explained by improved solubility or delayed desorption from plastic surfaces. In contrast, storage at 20 °C leads to a clear and reproducible loss of the ac^{4}C signal. After six months at 20 °C, less than 25% of the initial amount remains.

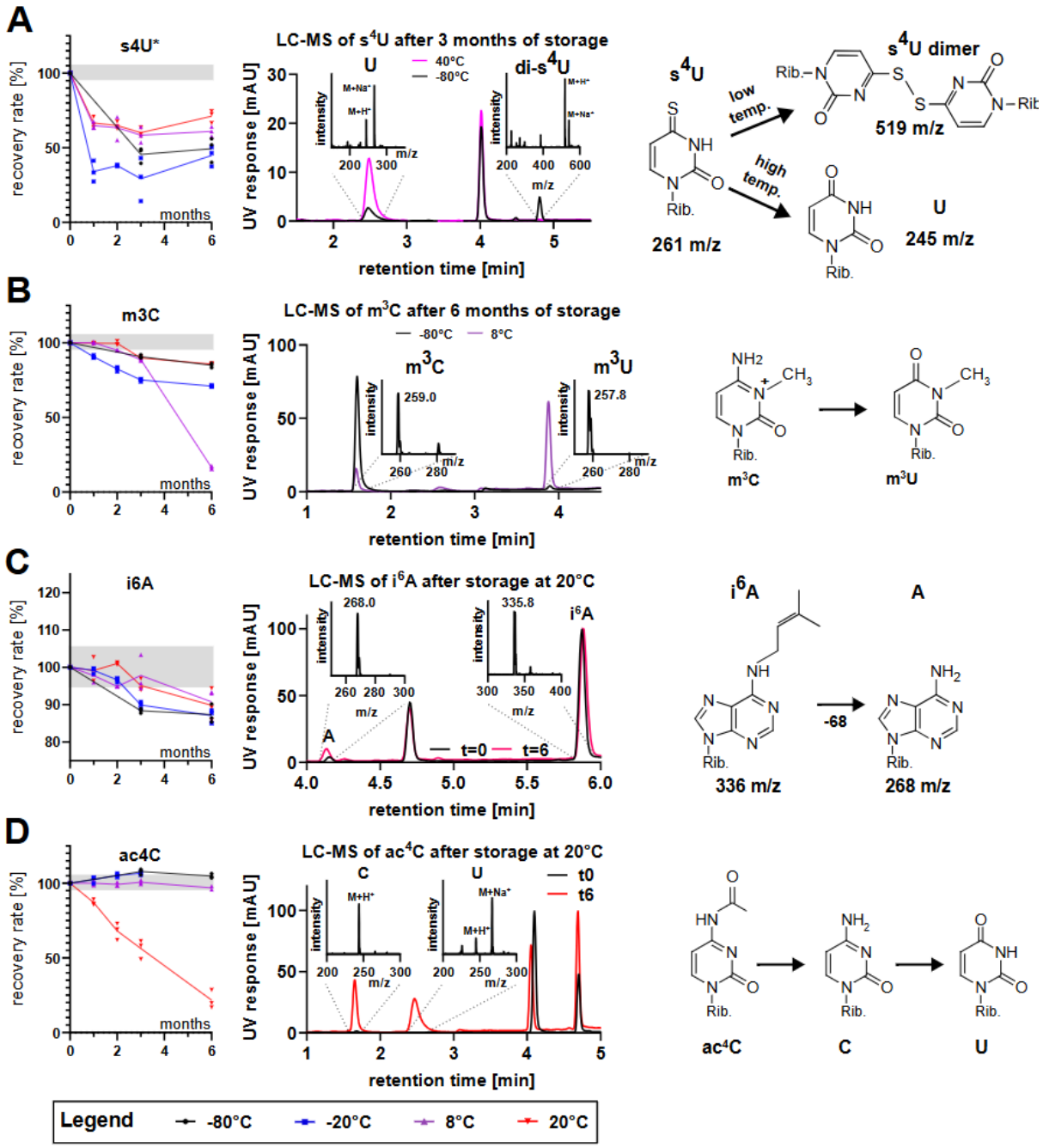

Figure 4 Temperature-dependent degradation of selected modified nucleosides. Color code xy-diagrams on left side: -80 °C (black), -20 °C (blue), 8 °C (purple) and 20 °C (red). Color code LC-MS chromatograms as indicated in respective figure. **(A)** Quantitative analysis and LC-UV-MS chromatograms of 4-thiouridine (s^4U) after storage at -80 °C (pink) and 40 °C (black) for three months. (B) Quantitative signal and LC-UV-MS chromatograms of 3-methylcytidine (m^3C) after storage at different temperatures for six months. (C) Quantitative profile and LC-UV-MS chromatograms of 6-isopentenyladenosine (i^6A) at initial and six-month time points. (D) Quantitative analysis and LC-UV-MS chromatograms of N4-acetylcytidine (ac^4C) after storage under varying temperature conditions for six months. All chromatograms correspond to samples stored at 20 °C for the indicated duration and are compared to freshly prepared reference samples (t = 0). Quantification was performed by LC-UV-MS.

Table 2 Important findings of this study

Nucleoside	**Quantification bias due to**	**Consequence**	**Solution**
All nucleosides	Evaporation of water over time	Actual concentration is higher than theoretical concentration ➔ underquantification	Monitor absorption every 6 months
m^2G, I, Im, ms^2t^6A, ms^2i^6A	Cause unknown	Abundance increases over time ➔ quantification bias	Prepare fresh solutions prior to analysis
$m^{6,6}A$ and m^6Am	Unproven hypothesis: Adhesion to polypropylene surface below 20 °C	Abundance drops over time ➔ overquantification	Prepare fresh or store at room temperature
s^4U	Chemical decomposition		Prepare fresh solutions prior to analysis
cm^5U, mcm^5U, ncm^5U and mcm^5Um	Chemical decomposition		Store at -20 °C
ac^4C	Chemical decomposition		Store below 8 °C
m^5U, m^5Um and m^7G, t^6A, m^6t^6A, m^6A	Chemical decomposition		Prepare fresh every 6 months and store at -80 °C
m^3C, m^1A, i^6A and mcm^5s^2U	Chemical decomposition		Prepare fresh every 3 months and store at -80 °C

LC-UV-MS analysis shows that ac^4C decays *via* a two-step hydrolytic pathway. In a first step, the acetyl group is lost, yielding cytidine (C), which subsequently undergoes deamination to

uridine (U). This transformation is confirmed by the appearance of new peaks at the retention times of C and U and their corresponding signals at *m/z* 244 and *m/z* 245, respectively. These results confirm that ac^{4}C is not stable in aqueous solution at ambient temperature, which has implications for the ongoing discussion on ac^{4}C presence in human mRNA which we will discuss later.

Hypermodified uridine derivatives show a particularly interesting behaviour in their degradation pathways. In Figure 5A the chromatogram of mcm^{5}s^{2}U shows the formation of 2 products. One with *m/z* 301 and one with *m/z* 317. These products form exclusively at 20 °C (Figure 5B). Using HRAMS (high resolution accuracy mass spectrometry), we identified the *m/z* 301 product to result from complete loss of Sulphur (Figure 5C). In addition to the intact nucleoside of this product, we identified a series of MS fragmentation products consistent with sequential loss of ribose and methyl group. This fragmentation pattern is in accordance with the fragmentation observed for the synthetic standard of mcm^{5}s^{2}U and mcm^{5}U. These species were observed with low mass deviations relative to the calculated theoretical values (less than 3 ppm), supporting accurate structural assignment. The value of HRAMS for such analyses becomes apparent in Figure 5D. A zoom into the *m/z* range of the M+2 range clearly indicates the presence of natural Sulphur-34 in mcm^{5}s^{2}U and absence of Sulphur-34 in the *m/z* 301 product, while both show the M+2 peak expected for natural Oxygen-18. The product with *m/z* 317 was more challenging as this mass is identical to the *m/z* of mcm^{5}U and in addition mcm^{5}U elutes at the retention time where the product *m/z* 317 was found. Only through HRAMS analysis, we could see that the product had a *m/z* of 317.2153 while mcm^{5}U has an *m/z* of 317.0984 (368 ppm error). Thus the identity of the second reaction product remains unclear.

For the hypermodified uridine derivative mcm^{5}Um we observed a cleavage of the ether leading to cm^{5}Um as the product. Interestingly, we did not observe this cleavage for mcm^{5}s^{2}U and mcm^{5}U (Figure S11). For ms^{2}i^{6}A, we observed a product with a mass increase of +16 Da (Figure S12). This might reflect the formation of known, native RNA modification ms^{2}io^{6}A, which requires further investigation.

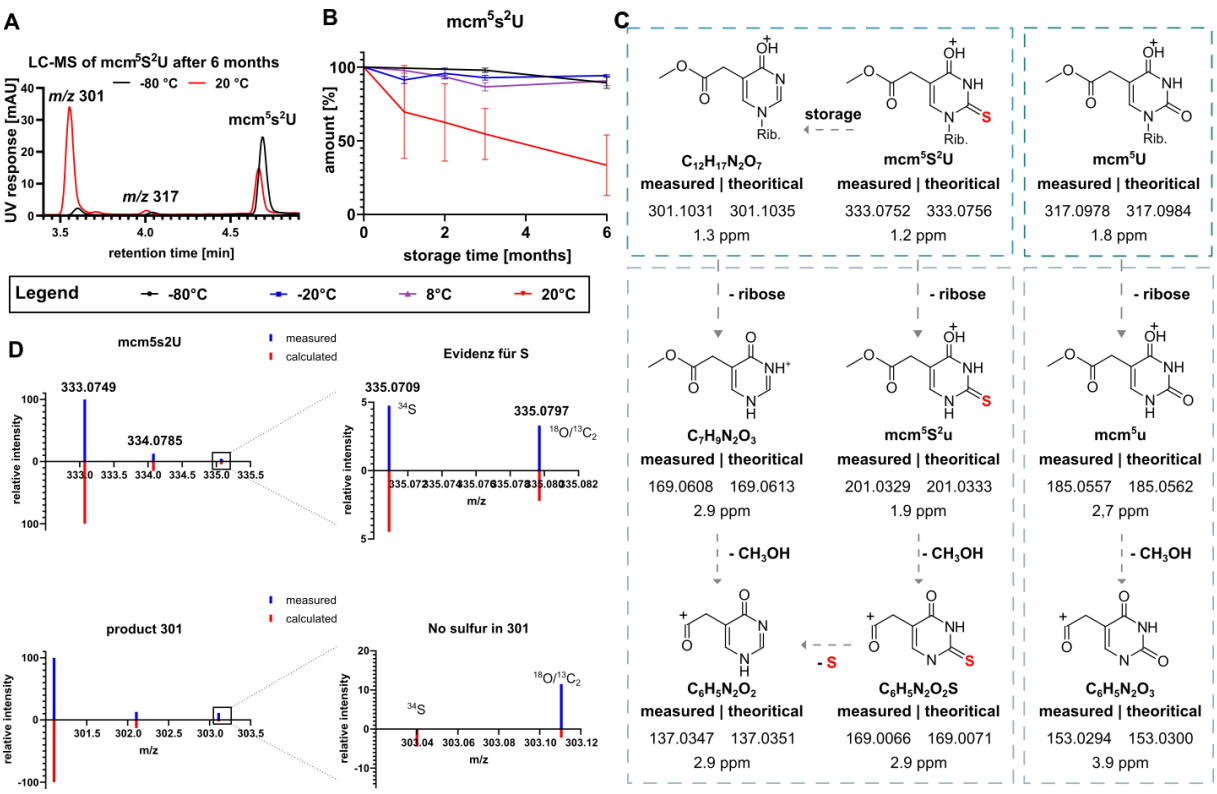

Figure 5 Degradation products of mcm^{5}s^{2}U (A) LC-UV-MS chromatograms of 5-methoxycarbonylmethyl-2-thiouridine (mcm^{5}s^{2}U) after storage at -80 °C (black) and 20 °C (red) for six months. **(B)** Quantitative analysis of mcm^{5}s^{2}U after storage for six months at -80 °C (black), -20 °C (blue), 8 °C (purple) and 20 °C (red). **(C)** HRAMS fragmentation pattern (including MS2 and MS3 scans) of mcm^{5}s^{2}U, product *m/z* 301 and mcm^{5}U. Mass deviation of suggested structures is indicated in ppm. **(D)** Isotopic pattern (^{13}C, ^{34}S, ^{18}O) of mcm^{5}s^{2}U and product with *m/z* 301. Values were measured by HRAMS and calculated based on the natural occurrence of isotopologues.

Theoretical analysis of degradation pathways

The degradation pathways for nucleosides analyzed here include (a) the deglycosylation reaction with water to yield the free nucleobase and ribofuranose; (b) the hydrolytic deamination of cytosine derivatives to yield the respective uracil bases and ammonia; (c) the hydrolytic deacetylation of 4-acetylaminocytosine derivatives to yield acetic acid and the respective cytosines; and (d) hydrolytic desulfurization of C2-thiocarbonyl derivatives of cytosine and uracil to yield hydrogen sulfide and the respective parent compounds. Reaction free energies (ΔG_{rxn}, in kJ mol^{-1}) for all four reaction types are obtained by subtracting the free energies ΔG_{298} of all reactants from those of the products. Results for the hydrolytic deglycosylation are collected in a graphical manner in Figure 6A. For most of the nucleosides studied here the deglycosylation reaction is endergonic by 3 - 11 kJ mol^{-1}. The sole exceptions

are the non-native 2-thiocarbonyl derivatives 2-thio-3-methylcytidine (**1rb2th3mC)** and 2-thio-3-methyluridine **1rb2th3mU** with small negative (-0.3 - -2.0 kJ mol^{-1}) reaction energies. It is, from a general point of view, comforting to see that reaction energies are least favorable for canonical nucleosides such as uridine (**1rbU)** and cytidine (**1rbC)**, which simply speaks for the stability of these systems.

The reaction free energies for the hydrolytic deamination of cytosine derivatives are collected for the full nucleoside as well as the respective free bases in Figure 6B. For cytidine (**1rbC**) and cytosine (**C**) as the reference systems of this group the deamination is moderately endergonic by 3.7 - 4.8 kJ mol^{-1}. While moderately exergonic reactions are predicted for some of the C5-substituted cytosine derivatives, the reaction becomes quite favorable for 3-methyl substituted cytosine derivatives. These may, depending on solution p*H* values, either be present in their neutral imino or protonated iminium ion form. For the neutral forms analyzed here the reaction energies amount to -26 - -31 kJ mol^{-1}. The impact of amino group protonation was studied in more detail for 3-methylcytosine (**3mC**) as the most relevant parent system. While hydrolytic deamination is exergonic by -30.5 kJ mol^{-1} for the neutral imino form shown in Figure 6B, the reaction energy is reduced to -19.5 kJ mol^{-1} for the protonated iminium ion form (see SI for details). Deamination is found to be least favorable for adenosine (**9rbA**) and its free base adenine (**A**). In more general terms, the deamination energetics of nucleosides and their free base equivalents are closely similar, which points to a rather limited influence of the N1 substituent on the deamination process.

Hydrolytic de-acetylation of cytosine derivatives carrying an acetyl group at the C4 amino group is exergonic for all nucleosides and nucleobases studied here (Figure 7A). The driving force for de-acetylation amounts to -10.2 kJ mol^{-1} for cytidine itself, which is in accordance with our experimental data described in Figure 4D. It becomes notably larger for C5-substituted cytidine derivatives. The most favorable reaction energy is found for the 5-methyl substituted system (**1rb4ac5mC**) with ΔG_{rxn} = -24.9 kJ mol^{-1}. These results open room for speculation: Is 4-acetyl-5-methylcytidine a non-natural RNA modification, or is it natural but due to its instability undetectable in current analytical systems?

Reaction energies for hydrolytic de-sulfurisation as the fourth degradation pathway analyzed here are shown in Figure 7B in a graphical manner. De-sulfurisation is found to be energetically favorable for all systems studied here with reaction energies ranging from -2.2 kJ mol^{-1} for 4-thiouridine (**1rb4thU)** to -23.0 mol^{-1} for the non-native 2-thio-3-methyluridine (**1rb2th3mU)**. De-sulfurisation energies differ, in selected cases, quite significantly between nucleosides and free bases. A point in case is 2-thiouridine (**1rb2thU)** the natural derivative of uridine with ΔG_{rxn} = -16.9 kJ mol^{-1} as compared to 2-thiouracil (**2thU)** with ΔG_{rxn} = -9.5 kJ mol^{-1}. Conformational analysis of the reactant and product nucleosides of the de-sulfurisation reaction indicates that

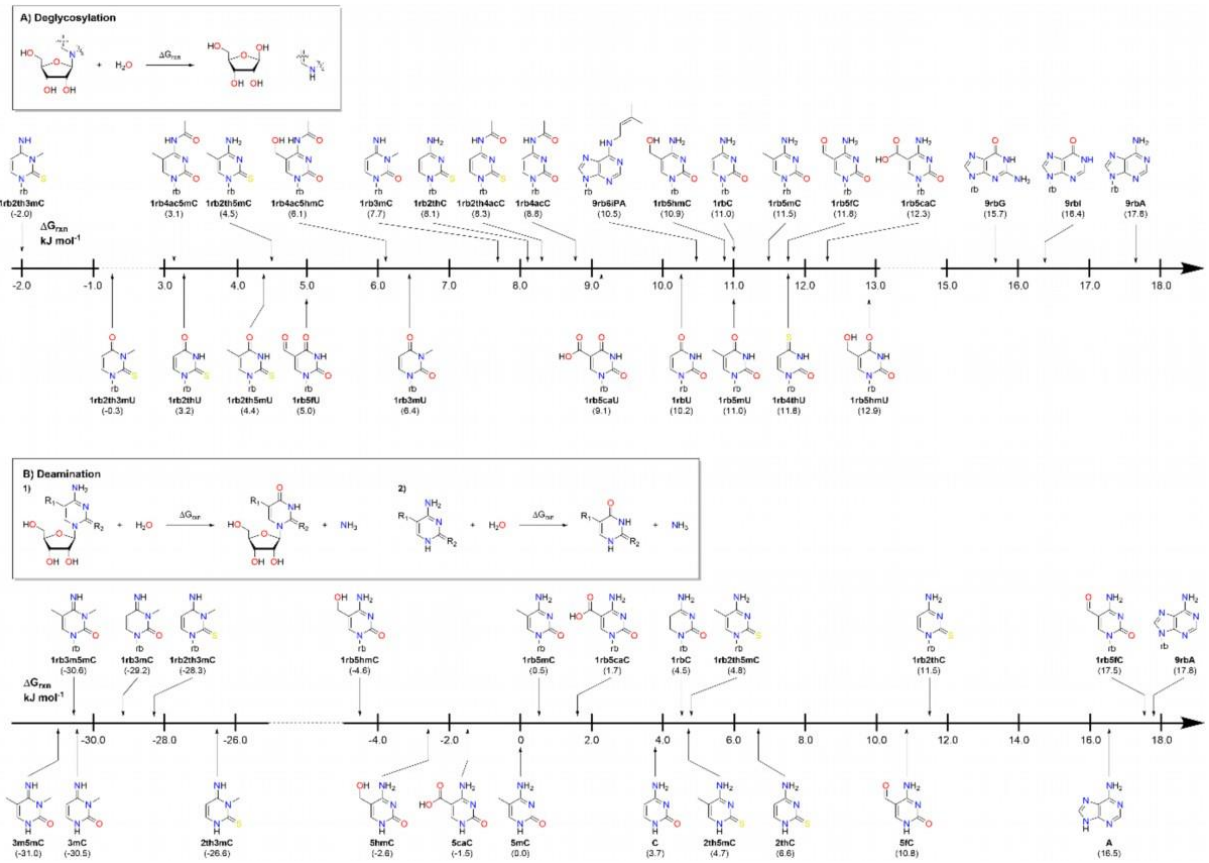

Figure 6. Reaction free energies for hydrolytic deglycosylation (A) and hydrolytic deamination (B) of different natural and non-natural nucleosides.

this is most likely due to differences in hydrogen bonding interactions between the ribosyl hydroxy substituents and the C2 carbonyl resp. thiocarbonyl group.

Finally, reaction energies were also calculated for the two competing pathways for the decomposition of s^4U shown in Figure 4A. For the free base of this latter system oxidative dimerization employing triplet oxygen as the reaction partner to yield the respective s^4U dimer and water as the products is highly exothermic at ΔG_{rxn} = -101.6 kJ/mol, whereas hydrolytic loss of sulfur is only marginally exergonic (ΔG_{rxn} = –3.8 kJ/mol). However, in dilute aqueous solution there is an abundance of water available as a reactant, while the availability of dissolved oxygen may, together with the requirement of radical-chain initiation, limit the role of oxidative dimerization. That the oxidative dimerization becomes less competitive at higher temperatures may also be due to the entropic requirements of a reaction turning three separate reactants into two products. This complex interplay of individual factors apparently generates a scenario, where both pathways coexist in parallel. The hydrolytic deprenylation of i^6A shown in Figure 4C is, in comparison, thermochemically quite unfavorable (with ΔG_{rxn} = +24.5 kJ/mol

for the nucleoside and +31.6 kJ/mol for the free base), which makes this process at least in the hydrolytic mechanism considered here quite unlikely.

All taken together, the calculation of reaction free energies for the four general degradation reactions analyzed here point to hydrolytic de-sulfurisation and hydrolytic de-acetylation is the more favorable degradation reactions, while hydrolytic deglycosilation is least favorable for all systems studied.

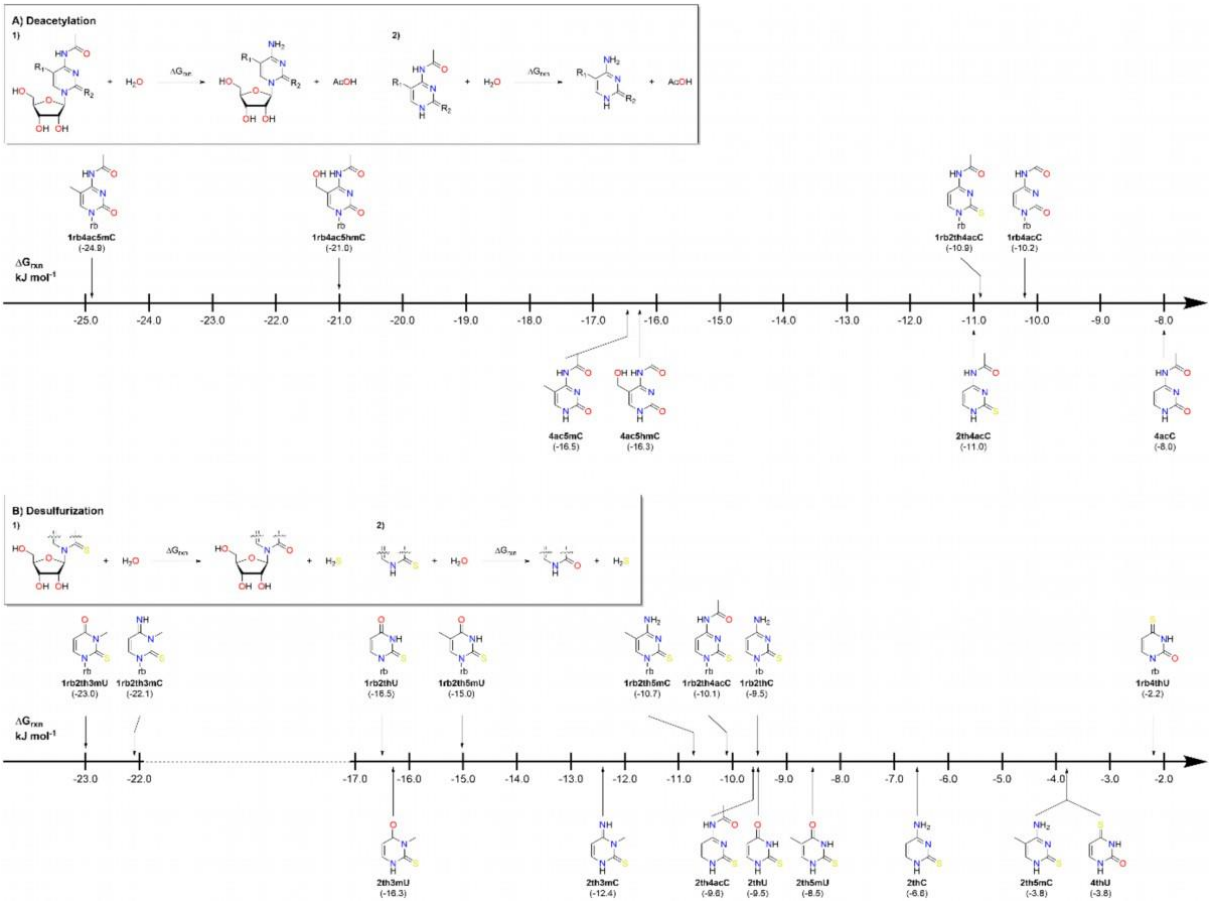

Figure 7. Reaction free energies for hydrolytic deacetylation (A) of C4-acetylated cytosine derivatives and hydrolytic de-sulfurisation of nucleosides and nucleobases with thiocarbonyl groups (B).

Discussion

This systematic survey of 44 nucleoside standards demonstrates that chemical stability in aqueous solution varies widely among RNA modifications and is strongly influenced by storage temperature. Canonical nucleosides and chemically inert derivatives remain quantitatively stable. In contrast, several labile modifications undergo distinct degradation reactions that are mechanistically consistent with the functional groups they carry. s^4U desulfurises or dimerises, m^3C and m^1A deaminate, ac^4C hydrolyses and deaminates, and mcm^5s^2U loses its Sulphur substituent. These pathways explain recurrent quantification artefacts that have been noted in routine LC-MS analyses and clarify conflicting reports in the epitranscriptomics literature, most notably the debate surrounding ac^4C in human mRNA. Several studies have reported widespread presence of ac^4C across coding regions, attributing functional relevance to this modification [37, 38]. However, more recent investigations, such as [39], have not detected ac^4C and attributed earlier findings to technical artefacts or misinterpretations. The pronounced chemical instability we observed for ac^4C in aqueous solution, especially its rapid deacetylation to cytidine and subsequent deamination to uridine, offers a unifying hypothesis: ac^4C may be genuinely present in mRNA but is lost prior to detection due to degradation during RNA preparation, handling, or storage. Thus, our results provide a compelling mechanistic explanation for the ongoing controversy surrounding the detection of ac^4C in human mRNA.

Physical effects introduce a second layer of bias. Evaporation during storage, even in sealed cryo-vials, and gradual release of analytes previously adsorbed to plasticware both inflate apparent concentrations. For chemically stable nucleosides the effect can exceed fifty percent after six months, whereas unstable modifications show superimposed signal loss governed by their intrinsic reactivity. Accurate quantification therefore requires a dual-control strategy: volumetric checks to correct for solvent loss and targeted monitoring of known degradation products. Another physical bias is observed for i^6A, m^2G, I, Im, m^6Am and $m^{66}A$ where we observe an increase in abundance that cannot be explained by evaporation alone. As no chemical process could generate these nucleosides in sealed storage, we interpret this effect as an apparent signal increase likely driven by physical factors, such as adsorption and temperature-dependent desorption from well or tube surfaces. An alternative explanation might be precipitation in some cases. We will follow up on these physical biases and find solutions for them that can be implemented in any analytical laboratory. These findings highlight a broader analytical concern in nucleoside quantification. Namely, that stability studies must consider not only degradation but also factors that may transiently influence apparent analyte abundance.

The present data cover the first six months of storage. Plates remain archived at -80 °C, -20 °C, 8 °C and 20 °C and will be analysed after 12, 24 and 36 months. These long-term

measurements will allow us to (i) resolve additional, slower decay channels, (ii) establish kinetic models that predict remaining analyte fractions for routine laboratory timelines, and (iii) refine guidance on maximum permissible storage intervals for each modification. In parallel, we are testing alternative containers and sealing materials, including fluoropolymer vials and glass inserts, to mitigate evaporation and adsorption artefacts. The resulting pragmatic workflow is expected to minimise both chemical degradation and physical concentration errors, thereby improving inter-laboratory comparability of quantitative RNA modification data.

Conflicts of interest

There are no conflicts to declare.

Acknowledgements

The authors would like to thank Jens Wöhnert and his working group for providing the instrument (NMR). Special thanks to Elke Duchardt-Ferner for her time, instructions and advice.

Data availability

The data supporting this article have been included as part of the Supplementary Information.

Funding

This work was funded by the Deutsche Forschungsgemeinschaft (325871075-SFB 1309 to S.K. and H.Z.). Stefanie Kaiser is a member of the human RNome Project Consortium.

References

1. Cappannini, A., et al., *MODOMICS: a database of RNA modifications and related information. 2023 update.* Nucleic Acids Res, 2024. **52**(D1): p. D239-D244.
2. Borowski, R., et al., *Novel entry to the synthesis of (S)- and (R)-5-methoxycarbonylhydroxymethyluridines - a diastereomeric pair of wobble tRNA nucleosides.* RSC Adv, 2019. **9**(69): p. 40507-40512.
3. Thumbs, P., et al., *Synthesis of Galactosyl-Queuosine and Distribution of Hypermodified Q-Nucleosides in Mouse Tissues.* Angewandte Chemie International Edition, 2020. **59**(30): p. 12352-12356.
4. Hillmeier, M., et al., *Synthesis and structure elucidation of the human tRNA nucleoside mannosyl-queuosine.* Nat Commun, 2021. **12**(1): p. 7123.
5. Meyer, B., et al., *Identification of the 3-amino-3-carboxypropyl (acp) transferase enzyme responsible for acp3U formation at position 47 in Escherichia coli tRNAs.* Nucleic Acids Res, 2019.
6. Nakanishi, K., et al., *Structure of the fluorescent Y base from yeast phenylalanine transfer ribonucleic acid.* Journal of the American Chemical Society, 1970. **92**(26): p. 7617-7619.
7. Kim, S., et al., *PubChem 2023 update.* Nucleic Acids Res, 2023. **51**(D1): p. D1373-D1380.

8. Grosjean, H., G. Keith, and L. Droogmans, *Detection and Quantification of Modified Nucleotides in RNA Using Thin-Layer Chromatography*, in *RNA Interference, Editing, and Modification: Methods and Protocols*, J.M. Gott, Editor. 2004, Humana Press: Totowa, NJ. p. 357-391.
9. Dunn, D.B., et al., *PURINES, PYRIMIDINES, NUCLEOSIDES, AND NUCLEOTIDES: PHYSICAL CONSTANTS AND SPECTRAL PROPERTIES*. 2010, CRC Press. p. 269-358.
10. Macon, J.B. and R. Wolfenden, *1-Methyladenosine. Dimroth rearrangement and reversible reduction.* Biochemistry, 1968. **7**(10): p. 3453-8.
11. Ammann, G., et al., *Pitfalls in RNA Modification Quantification Using Nucleoside Mass Spectrometry.* Acc Chem Res, 2023. **56**(22): p. 3121-3131.
12. Alseth, I., B. Dalhus, and M. Bjørås, *Inosine in DNA and RNA.* Current Opinion in Genetics & Development, 2014. **26**: p. 116-123.
13. Bessler, L., et al., *Reversible oxidative dimerization of 4-thiouridines in tRNA isolates.* RSC Chem Biol, 2024. **5**(3): p. 216-224.
14. Jora, M., et al., *Chemical Amination/Imination of Carbonothiolated Nucleosides During RNA Hydrolysis.* Angewandte Chemie International Edition, 2021. **60**(8): p. 3961-3966.
15. Matuszewski, M., et al., *A hydantoin isoform of cyclic N6-threonylcarbamoyladenosine (ct6A) is present in tRNAs.* Nucleic Acids Research, 2016. **45**(4): p. 2137-2149.
16. Miyauchi, K., S. Kimura, and T. Suzuki, *A cyclic form of N6-threonylcarbamoyladenosine as a widely distributed tRNA hypermodification.* Nat Chem Biol, 2013. **9**(2): p. 105-11.
17. Bessler, L., et al., *Esterification of Cyclic N6-Threonylcarbamoyladenosine During RNA Sample Preparation.* ChemMedChem, 2024. **19**(13): p. e202400115.
18. Pracht, P., F. Bohle, and S. Grimme, *Automated exploration of the low-energy chemical space with fast quantum chemical methods.* Phys Chem Chem Phys, 2020. **22**(14): p. 7169-7192.
19. Grimme, S., *Exploration of Chemical Compound, Conformer, and Reaction Space with Meta-Dynamics Simulations Based on Tight-Binding Quantum Chemical Calculations.* J Chem Theory Comput, 2019. **15**(5): p. 2847-2862.
20. Bannwarth, C., S. Ehlert, and S. Grimme, *GFN2-xTB-An Accurate and Broadly Parametrized Self-Consistent Tight-Binding Quantum Chemical Method with Multipole Electrostatics and Density-Dependent Dispersion Contributions.* J Chem Theory Comput, 2019. **15**(3): p. 1652-1671.
21. Becke, A.D., *A new mixing of Hartree–Fock and local density-functional theories.* The Journal of Chemical Physics, 1993. **98**(2): p. 1372-1377.
22. Grimme, S., et al., *Dispersion-Corrected Mean-Field Electronic Structure Methods.* Chemical Reviews, 2016. **116**(9): p. 5105-5154.
23. Weigend, F. and R. Ahlrichs, *Balanced basis sets of split valence, triple zeta valence and quadruple zeta valence quality for H to Rn: Design and assessment of accuracy.* Phys Chem Chem Phys, 2005. **7**(18): p. 3297-305.
24. Marenich, A.V., C.J. Cramer, and D.G. Truhlar, *Universal Solvation Model Based on Solute Electron Density and on a Continuum Model of the Solvent Defined by the Bulk Dielectric Constant and Atomic Surface Tensions.* The Journal of Physical Chemistry B, 2009. **113**(18): p. 6378-6396.
25. Gaussian 09, Revision D.01, M. J. Frisch, G. W. Trucks, H. B. Schlegel, G. E. Scuseria, M. A. Robb, J. R. Cheeseman, G. Scalmani, V. Barone, B. Mennucci, G. A. Petersson, H. Nakatsuji, M. Caricato, X. Li, H. P. Hratchian, A. F. Izmaylov, J. Bloino, G. Zheng, J. L. Sonnenberg, M. Hada, M. Ehara, K. Toyota, R. Fukuda, J. Hasegawa, M. Ishida, T. Nakajima, Y. Honda, O. Kitao, H. Nakai, T. Vreven, J. A. Montgomery, Jr., J. E. Peralta, F. Ogliaro, M. Bearpark, J. J. Heyd, E. Brothers, K. N. Kudin, V. N. Staroverov, T. Keith, R. Kobayashi, J. Normand, K. Raghavachari, A. Rendell, J. C. Burant, S. S. Iyengar, J. Tomasi, M. Cossi, N. Rega, J. M. Millam, M. Klene, J. E. Knox, J. B. Cross, V. Bakken, C. Adamo, J. Jaramillo, R. Gomperts, R. E. Stratmann, O. Yazyev, A. J. Austin, R. Cammi, C. Pomelli, J. W. Ochterski, R. L. Martin, K. Morokuma, V. G. Zakrzewski, G. A. Voth, P. Salvador, J. J. Dannenberg, S. Dapprich, A. D. Daniels, O. Farkas, J. B. Foresman, J. V. Ortiz, J. Cioslowski, and D. J. Fox, Gaussian, Inc., Wallingford CT, **2013**.

26. Altun, A., F. Neese, and G. Bistoni, *Local energy decomposition analysis of hydrogen-bonded dimers within a domain-based pair natural orbital coupled cluster study.* Beilstein Journal of Organic Chemistry, 2018. **14**: p. 919-929.
27. Saitow, M., et al., *A new near-linear scaling, efficient and accurate, open-shell domain-based local pair natural orbital coupled cluster singles and doubles theory.* The Journal of Chemical Physics, 2017. **146**(16).
28. Dunning, T.H., Jr., *Gaussian basis sets for use in correlated molecular calculations. I. The atoms boron through neon and hydrogen.* The Journal of Chemical Physics, 1989. **90**(2): p. 1007-1023.
29. Neese, F. and E.F. Valeev, *Revisiting the Atomic Natural Orbital Approach for Basis Sets: Robust Systematic Basis Sets for Explicitly Correlated and Conventional Correlated ab initio Methods?* Journal of Chemical Theory and Computation, 2011. **7**(1): p. 33-43.
30. Fu, Y., et al., *The AlkB Domain of Mammalian ABH8 Catalyzes Hydroxylation of 5-Methoxycarbonylmethyluridine at the Wobble Position of tRNA.* Angewandte Chemie International Edition, 2010. **49**(47): p. 8885-8888.
31. van den Born, E., et al., *ALKBH8-mediated formation of a novel diastereomeric pair of wobble nucleosides in mammalian tRNA.* Nature Communications, 2011. **2**(1): p. 172.
32. Malz, F. and H. Jancke, *Validation of quantitative NMR.* J Pharm Biomed Anal, 2005. **38**(5): p. 813-23.
33. Weber, M., et al., *Using high-performance (1)H NMR (HP-qNMR(R)) for the certification of organic reference materials under accreditation guidelines--describing the overall process with focus on homogeneity and stability assessment.* J Pharm Biomed Anal, 2014. **93**: p. 102-10.
34. Schoenberger, T., *Determination of standard sample purity using the high-precision 1H-NMR process.* Anal Bioanal Chem, 2012. **403**(1): p. 247-54.
35. Barraud, P., et al., *Time-resolved NMR monitoring of tRNA maturation.* Nat Commun, 2019. **10**(1): p. 3373.
36. Heiss, M., et al., *Cell culture NAIL-MS allows insight into human tRNA and rRNA modification dynamics in vivo.* Nat Commun, 2021. **12**(1): p. 389.
37. Arango, D., et al., *Acetylation of Cytidine in mRNA Promotes Translation Efficiency.* Cell, 2018. **175**(7): p. 1872-1886 e24.
38. Liu, S., et al., *Uncovering N4-Acetylcytidine-Related mRNA Modification Pattern and Landscape of Stemness and Immunity in Hepatocellular Carcinoma.* Front Cell Dev Biol, 2022. **10**: p. 861000.
39. Georgeson, J. and S. Schwartz, *No evidence for ac4C within human mRNA upon data reassessment.* Mol Cell, 2024. **84**(8): p. 1601-1610 e2.